Stray light evaluation for the Astrometric Gravitation Probe mission

Landini Federico[a], Riva Alberto[b], Gai Mario[b], Baccani Cristian[c], Focardi Mauro[a], and Pancrazzi Maurizio[a]

[a]INAF - Osservatorio Astrofisico di Arcetri, Largo E. Fermi 5, Firenze, Italy
[b]INAF - Osservatorio Astrofisico di Torino, Strada Osservatorio 20, Pino Torinese, Italy
[c]Università degli Studi di Firenze - Dipartimento di Fisica e Astronomia, Via Sansone 1, Sesto Fiorentino, Italy

ABSTRACT

The main goal of the Astrometric Gravitation Probe mission is the verification of General Relativity and competing gravitation theories by precise astrometric determination of light deflection, and of orbital parameters of selected Solar System objects. The key element is the coherent combination of a set of 92 circular entrance apertures, each feeding an elementary inverted occulter similar to the one developed for Solar Orbiter/METIS.[1] This provides coronagraphic functions over a relevant field of view, in which all stars are observed for astrometric purposes with the full resolution of a 1 m diameter telescope. The telescope primary mirror acts as a beam combiner, feeding the 92 pupils, through the internal optics, toward a single focal plane. The primary mirror is characterized by 92 output apertures, sized according to the entrance pupil and telescope geometry, in order to dump the solar disk light beyond the instrument. The astronomical objects are much fainter than the solar disk, which is angularly close to the inner field of view of the telescope. The stray light as generated by the diffraction of the solar disk at the edges of the 92 apertures defines the limiting magnitude of observable stars. In particular, the stray light due to the diffraction from the pupil apertures is scattered by the telescope optics and follows the same optical path of the astronomical objects; it is a contribution that cannot be eliminated and must therefore be carefully evaluated. This paper describes the preliminary evaluation of this stray light contribution.

Keywords: General Relativity, AGP, Astrometry, Stray light, Diffraction, BRDF

1. INTRODUCTION

One of the major challenges of today's Fundamental Physics is the merging of Einstein's General Relativity (GR), the reference theory on macroscopic scale, with Quantum Mechanics (QM), which describes with extreme precision the behavior of elementary particles. Their combination in a Unified Theory will require profound modification of either or both of them; it is therefore of paramount importance to test them to a level in which significant deviations may be detected, in order to set the experimental constraints for the future overarching models.

The Astrometric Gravitation Probe (AGP) is the concept of a space mission based on coronagraphy and high precision astrometry aimed at testing GR and competing gravitation theories, in particular with respect to the γ and β parameters of the Parametrized Post-Newtonian (PPN) formulation of weak field gravity models,[2] by measurement of the light deflection and Solar System Ephemerides.

The 1919 eclipse experiment of Eddington, Dyson and Davidson[3] reached a precision of about 10% on light deflection, hence on the PPN parameter γ, and provided the most popular demonstration of GR's prediction capability.

Subsequent tests during the past century did not improve significantly on such precision, since eclipses usually have short duration, happen in locations not endowed with large telescopes (thus requiring small, portable, equipment), and suffer from the high background flux from the solar corona, as well as from atmospheric disturbances. GR also successfully justified the previously unexplained excess perihelion shift of Mercury, known since

Further author information: (Send correspondence to F.L.)
F.L.: E-mail: flandini@arcetri.astro.it, Telephone: +39 (0)55 275 5221

Optical and Infrared Interferometry and Imaging V, edited by Fabien Malbet, Michelle J. Creech-Eakman, Peter G. Tuthill, Proc. of SPIE Vol. 9907, 990741
 · doi: 10.1117/12.2232568

the mid of XIX century, and related to an algebraic combination of γ and β.
Modern tests, based on a range of techniques, reach a precision of order of a few 10^{-5} on γ[4,5] and β,[6,7] with the perspective of improving by about one order of magnitude in the near future thanks to the results of respectively Gaia[8,9] on γ, and Solar Orbiter[10] and BepiColombo[11] on β.

AGP, thanks to an optimized design of satellite and operation, will take advantage of the techniques demonstrated by Gaia and Solar Orbiter to improve by at least an additional order of magnitude on both γ and β PPN parameters. An experiment located in space is able to overcome the limitations of the 1919 eclipse experiment, implementing a permanent eclipse by coronagraphic techniques and achieving sub-milliarcsec (mas) precision on a sample of several million stars down to V = 16 mag in a $\pm 1^\circ$ strip along the Ecliptic plane. The amplitude of light deflection in this region is ~ 0.5 arcsec. The combination of coronagraphy, high sensitivity and good angular resolution is achieved by combination of the inverted coronagraph concept[1] and of Fizeau interferometry, i.e. aperture masking, on a 1 m class telescope with large field of view.[12]
The AGP payload / operation design (described in section 2) is focused on the minimization of systematic errors, in particular through the measurement of symmetry constraints. The observation in opposition to the Sun provides an astrometric calibration on the stars and additional orbital points on the selected Solar system objects used for the determination of β. This is achieved by a "rear-viewing" mirror included in the payload design (section 2.3), for simultaneous measurement of both deflected and undeflected sources.
Since the instrument has coronagraphic capabilities, it faces the critical issues typical of many other solar coronagraphs, in particular, stray light rejection requirements. The stray light requirement is comparably soft, since it affects the limiting magnitude of the stellar sample, but the impact of higher background on the deflection estimate is a graceful degradation of performance. Stars significantly brighter than the limiting magnitude are photon limited, and provide the most relevant contribution to the astrometric precision budget. Lower background values allow observation of a much larger population of fainter stars, having an intrinsically larger astrometric error due to their lower photon flux. The mission performance estimate was computed also as a function of the stray light, evidencing a limiting magnitude between V=15 mag and V=17 mag for a background level ranging between 6,000 and 6 photo-electrons/s per pixel, approximately. The background includes stray light from the solar disk and actual coronal emission.
The entrance aperture is directly hit by the solar disk and constitutes the main stray light source. In fact, the solar disk light diffracted by the entrance aperture and scattered by the optics follows the same path of the stars signal and is collected on the focal plane. It is a contribution that shall be calculated and compared with the expected signal. This paper is dedicated to the description of the preliminary theoretical evaluation of the stray light on the focal plane as generated by diffraction of the solar disk light. Section 3 is dedicated to the stray light analysis description.

2. OPTICAL DESIGN OVERVIEW

The AGP telescope is designed[12] with two channels (16 x 16 arcmin each) pointing symmetrically at about $\pm 1^\circ$ with respect to the optical axis of the telescope, which is set on the solar disk center. Each channel has a similar and symmetric layout with respect to the telescope optical axis.
The 3D optical layout of AGP is shown in Fig. 1. We can schematize the optical design as made of two stages, the first with a common optical path, the second with two separate paths. The first stage (section 2.1 is constituted by the pupil mask, PM, the primary mirror, M1, and the secondary mirror, M2. The folding mirrors, M3, separate the two fields of view (section 2.2).
The so-called rear-view mirror provides an additional feature to the AGP design and is described in section 2.3.

2.1 The first stage

The PM is the entrance element, a disk with a set of 92 circular apertures, drilled in three coronae differently populated as shown in Fig. 2. The M1 is an annular concave mirror positioned at a distance of 1750 mm from the PM. It is characterized by 92 circular apertures, positioned in correspondence of the elementary apertures on the PM. The apertures function is to dump to space the photon flux from the solar disk; their size is defined in order to cope with the solar disk divergence (16 arcmin at 1 AU).
M2 is a convex mirror, that directs the optical path toward the central open area of M1, where the two channels are split by the two folding mirrors (M3, one per channel).

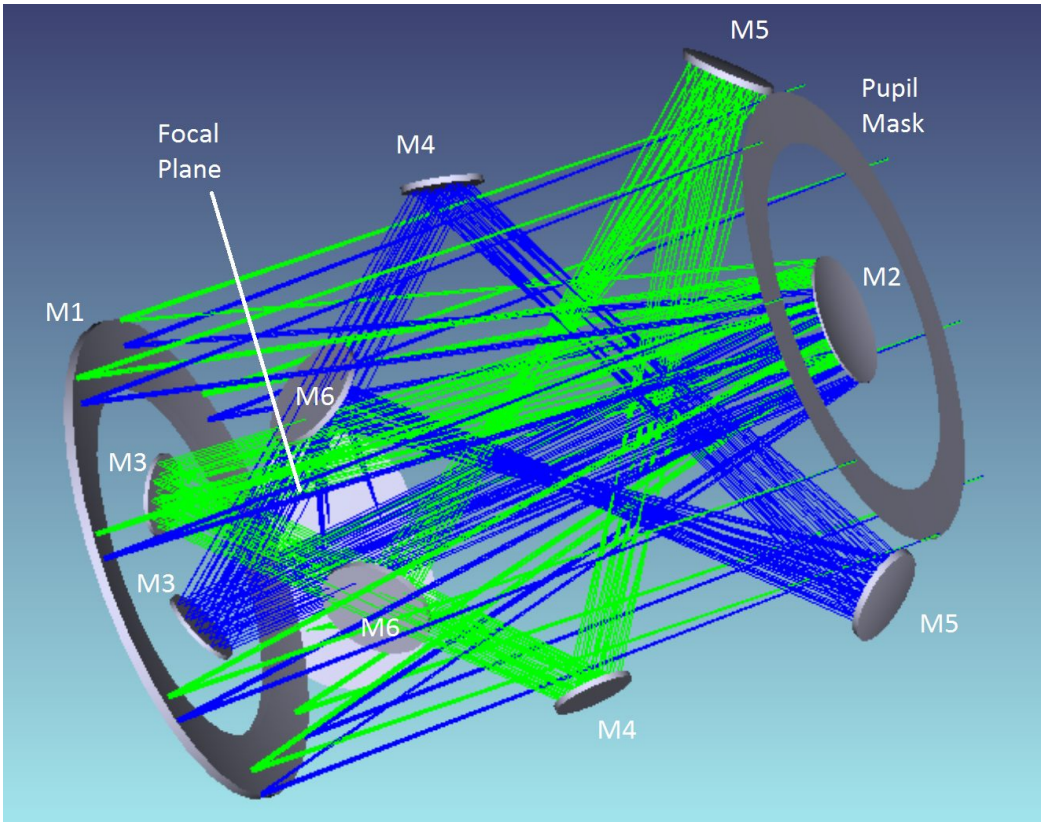

Figure 1. 3D Optical layout of AGP.

2.2 The second stage

The two M3s are tilted symmetrically with respect to the optical axis.
Figure 3 shows the path of both channels at the same time (blue-green). Then, the beam is further folded by the two M4s towards the off axis mirrors M5. The beam reflected by the M5s is bent by the M6s in the plane perpendicular to the optical axis towards the focal plane. The M6s placement is anti-symmetric with respect to the channels separation, since their task is to combine the light coming from the two fields into a single focal plane.
The common focal plane "re-combines" the two channels, providing a superposed image of the two fields of view. This superposition is necessary for the calibration process, which is crucial for the AGP measurements.
The focal plane of AGP will be populated by 32 CCDs (2k x 4k with pixel size of 10 μm). The mosaic has a complexity comparable to those of Gaia[13] and Euclid.[14] We foresee the presence of some proximity boards to drive the CCD and receive the output data, while the data processing unit will be positioned farther away in a service module.

2.3 The rear-view mirror

A peculiar characteristic of the AGP design is the rear-view mirror. The rear-view mirror, fed through the apertures on the M1, allows repeated measurements of the same stellar sample in conditions of maximum and minimum deflection, in order to get rid of systematic errors.
It is a flat annular mirror with a set of 92 holes properly resized, in order to provide clearance for the main optical path through the PM.
Figure 4 shows in red the position of the rear-view mirror. According to AGP measurements principles, star light coming from sources in the direction opposite to the Sun, are not affected by any deflection, and should

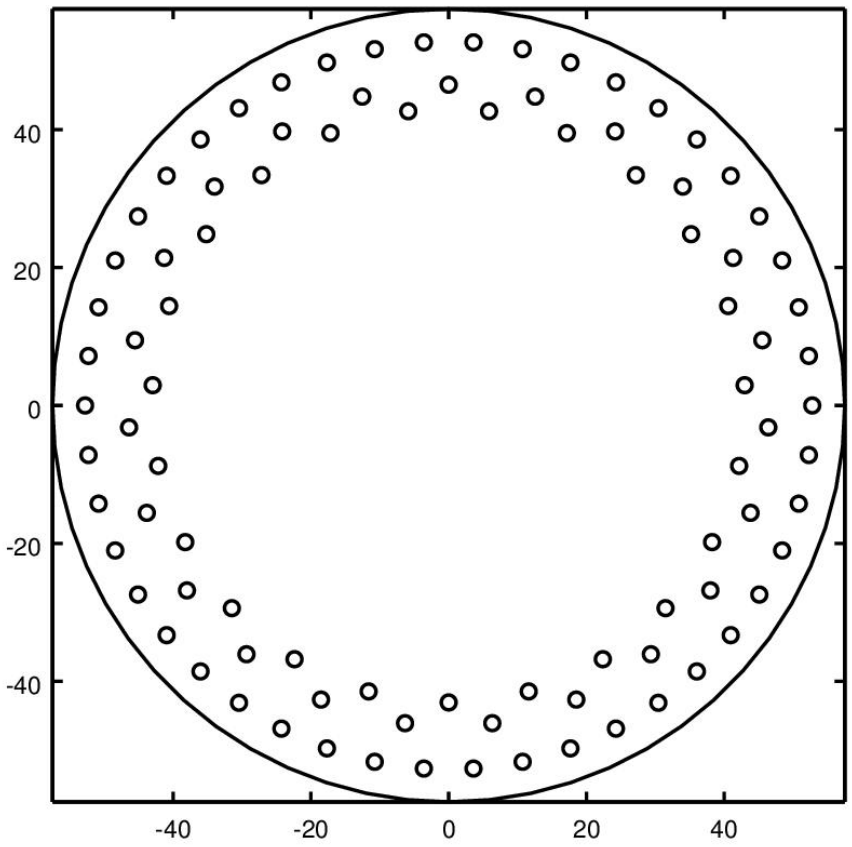

Figure 2. Scheme of the 92 circular apertures drilled in the PM. Units are cm.

improve the calibration issues of the experiment. Therefore, the focal plane will simultaneously contain images the two front and the two rear fields of view.

3. STRAY LIGHT PRELIMINARY EVALUATION

The PM is directly hit by the solar disk light, thus it constitutes the main stray light source for a coronagraphic system such as AGP.
The light diffracted by the 92 PM apertures is reflected and scattered first by the M1 and then by the other telescope optics. Since the optics that follow the M1 in the optical path (see section 2) process a stray light contribution that is several order of magnitude lower with respect to the light diffracted by the PM, we assume that their contribution to the total level of stray light on the focal plane is negligible with respect to the M1 contribution. Within this hypothesis, the stray light as evaluated on the primary focal plane is an indicative estimate of the stray light level we may expect on the telescope focal plane.
The stray light on the primary focal plane is calculated according to the following steps, that are based on different physical principles and are thoroughly described in the next subsections:

- evaluation of the diffraction due to the PM apertures on the M1 surface, taking into account the whole solar disk as a source (section 3.1);

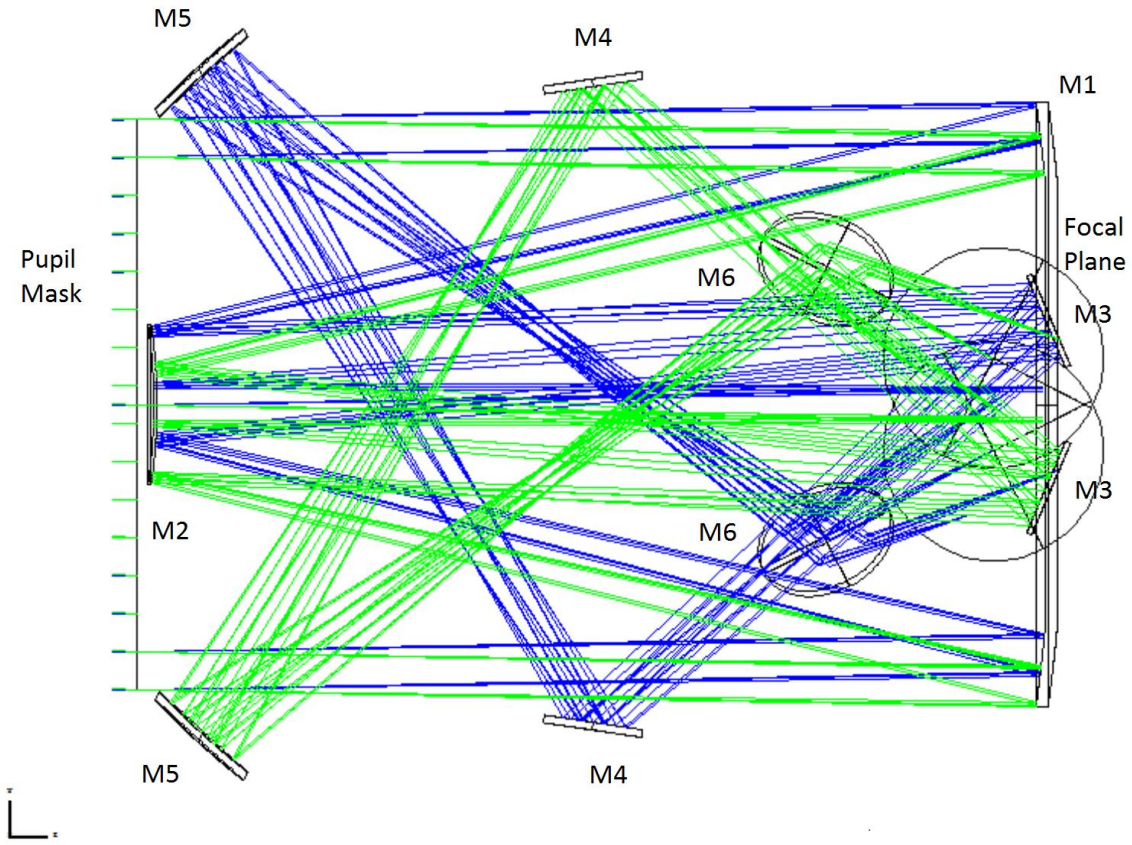

Figure 3. Optical layout of AGP for the two channels (North-South).

- propagation of the diffraction from the M1 plane down to the primary focal plane taking into account both the reflection and the scattering due to the mirror surface micro-roughness (section 3.2).

3.1 Diffraction evaluation on the primary mirror plane

The diffraction pattern on the M1 plane is calculated according to the following steps:

1. calculation of the diffraction produced by a single PM knife edge aperture on the M1 plane for a point source in the center of the solar disk (impinging plane wave parallel to the PM plane).
2. Convolution of the diffraction of step (1) with a solar disk kernel with the dimension of the solar disk on the M1 plane, in order to calculate the diffraction with the whole solar disk as a source, normalized to the mean solar disk brightness. The calculation is performed at a fixed wavelength (500 nm). The kernel includes a wavelength-dependent limb darkening model.[15]
3. Replication and 3D superposition of the diffraction pattern evaluated at step (2) according to the map of the 92 apertures.

The Fresnel diffraction as generated by a knife edge aperture for a single point source in the center of the solar disk (step 1) is calculated by means of the Fresnel-Kirchhoff theory:[16]

$$D_p(r,\lambda) = |U(r,\lambda)|^2 \simeq \left| \frac{-2Ai}{\lambda} \frac{e^{ikz}}{z} \iint_S e^{ik\frac{\xi^2+\eta^2}{2z}} d\xi d\eta \right|^2 \quad (1)$$

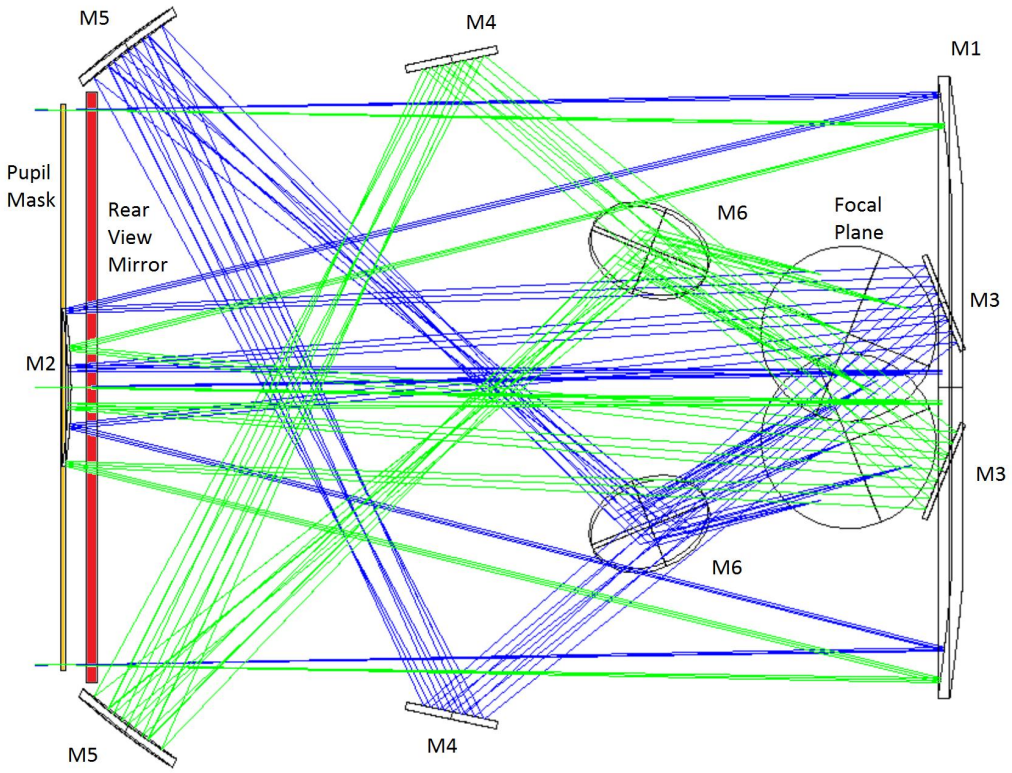

Figure 4. Optical layout of AGP for two channels, with the rear-view mirror (in red).

where $U(r, \lambda)$ is the value of the electro-magnetic field at a radial distance r on the image plane (the diffraction pattern for a single aperture on the PM has a circular symmetry), S is the integration surface on the diffracting plane, λ=550 nm is the wavelength, z=1750 mm is the distance between the PM and the M1 plane, η and ξ are orthonormal coordinates on the PM plane. In order to retrieve equation (1), a source at infinity has been considered, the close field approximation has been adopted and the origin of the frame of reference has been set at the intersection of the source-image point line with the aperture on the PM plane. The relative optical axis (ROA) of this sub-calculation is defined as the line that originates in the center of the PM aperture and is perpendicular to the PM plane. The radial coordinate r has its origin on the optical axis.
The resulting pattern is convolved (step (2)) with a solar disk kernel with the dimension of the solar disk as projected on the M1 plane:

$$D(r, \lambda) = B \int_0^{2\pi} d\hat{\phi} \int_0^{R_{Disk}} D_p(r - \rho, \hat{\phi} - \phi, \lambda) Disk(\rho, \phi, \lambda) \rho d\rho \tag{2}$$

where R_{Disk} is the radius of the projection of the solar disk on the M1 plane; $Disk(\rho, \phi, \lambda) = Disk(\rho, \lambda)$ is the circularly symmetric function that defines the irradiance of the solar disk at a given wavelength λ; it is 0 for ρ greater than the projection of the solar radius on the M1 plane. B is a normalization constant.
The following limb darkening model is included in the expression of $Disk(\rho, \lambda)$:[15]

$$L(\theta, \lambda) = 1 - u_2(\lambda) - v_2(\lambda) + u_2(\lambda) \cos\theta + v_2(\lambda) \cos^2\theta \tag{3}$$

where θ is the angle between the solar radius vector and the line of sight, while u_2 and v_2 are tabulated wavelength-dependent parameters.[15]
Each of the 92 apertures on the PM generates the diffraction pattern $D(r, \lambda)$ on the M1 plane, with a center of

symmetry defined by the intersection of the ROA with the M1 plane. A superposition is performed of the 92 diffraction patterns.
Figure 5 shows the resulting diffraction pattern on the M1 plane. The diffraction is quite symmetrically distributed around the apertures on the M1, which allows us to identify a profile along the yellow path in Fig. 5 as indicative of the diffraction level on the M1 plane. The diffraction along the yellow path evidenced in Fig. 5 is shown in Fig. 6.

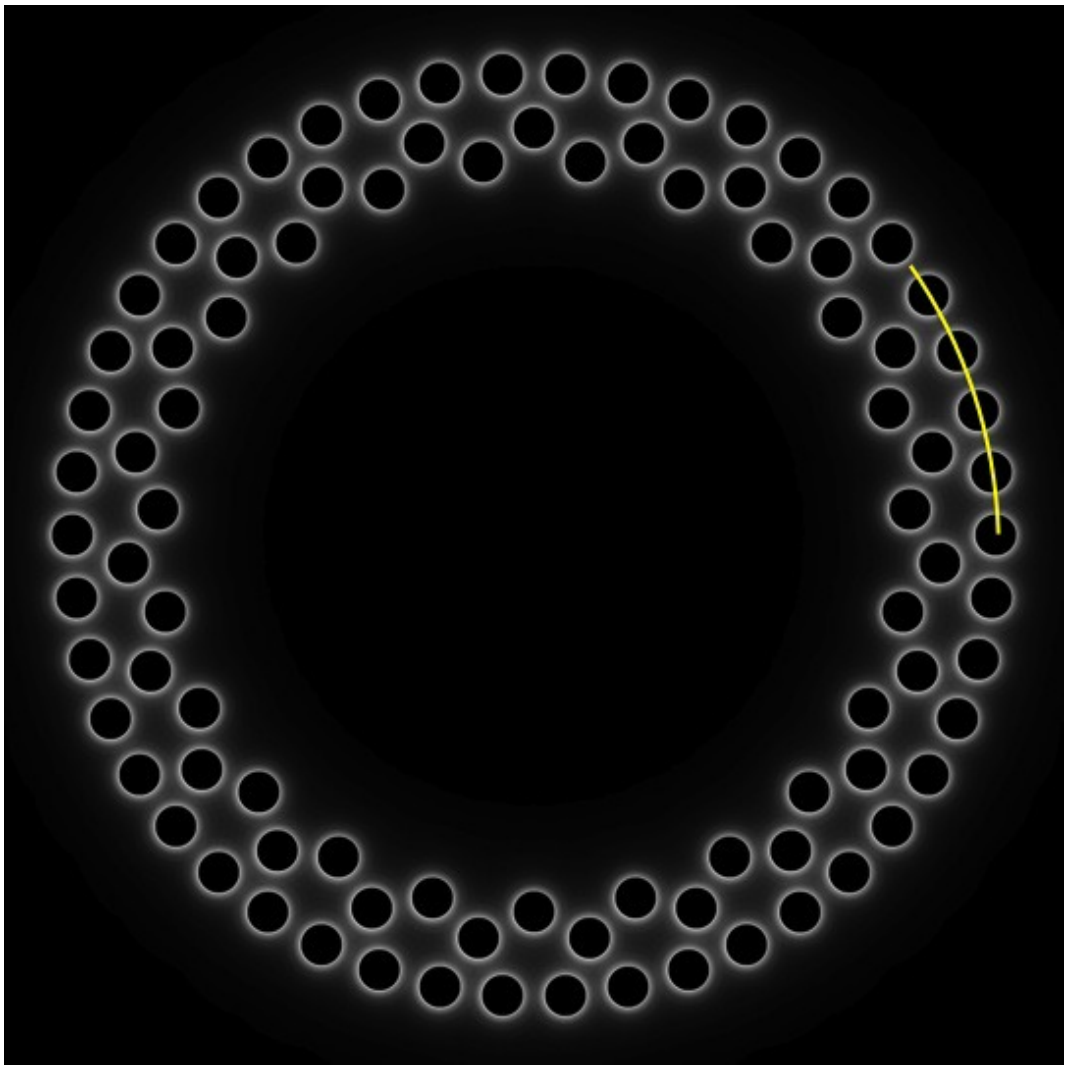

Figure 5. Diffraction pattern on the M1 plane, as generated by the 92 apertures of the PM, for the whole solar disk as a source.

3.2 Stray light on the primary focal plane

The M1 works as a beam combiner, feeding the primary focal plane with an overlapping of the contributions due to the mirror portions around each aperture.
The function of the M1 justifies the approach of estimating the stray light by propagating the diffraction distribution around one aperture only, multiplied by 92 (the number of apertures).
For the propagation, we select one of the diffraction profiles shown in Fig. 6.
Due to its micro-roughness, the M1 surface scatters the energy of each impinging ray within a cone, that has the

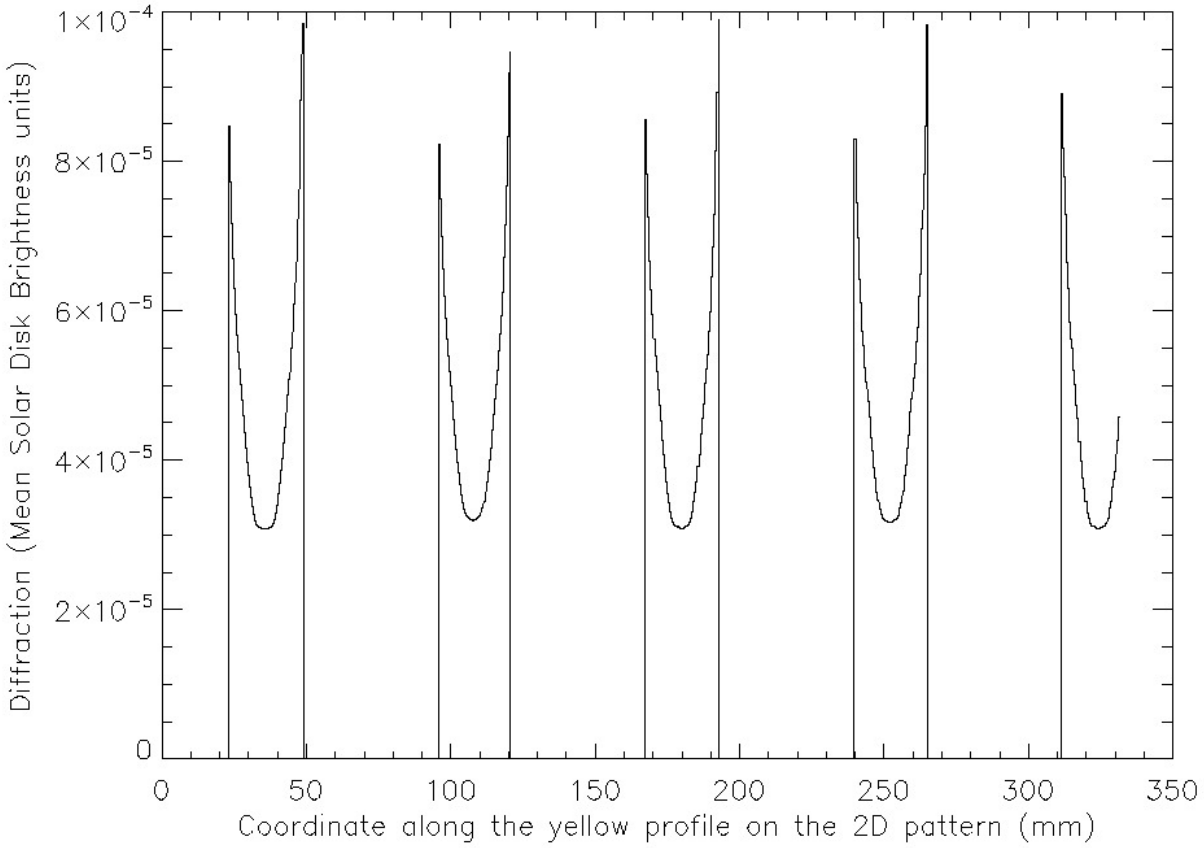

Figure 6. Profile of the diffraction along the yellow path evidenced in Fig. 5.

specularly reflected ray as its symmetry axis.
A super-polished mirror surface is characterized by a micro-roughness, σ, and an auto-correlation length, ζ, that define the scattering characteristics of the surface:

- total integrated scatter, $\mathrm{TIS} = (4\pi\sigma/\lambda)^2$, which is the ratio between the total scattered flux and the total reflected flux.
- Bidirectional-scatter distribution function (BRDF), the angular distribution of the scattered light with respect to the incident light, which can be modelled by means of a Lorentzian function of this kind:[17,18]

$$\mathrm{BRDF}(\theta) \simeq \mathrm{TIS} \cdot \frac{1}{2\pi} \cdot \frac{(2/\theta_0)^2}{[1+(2\theta/\theta_0)^2]^{3/2}} \quad , \tag{4}$$

  where θ is the angle formed by the scattered ray and the reflected ray, and θ_0 is the characteristic width of the distribution.

In order to evaluate the total amount of stray light that impinges on the detector, we consider the scattering off the M1 surface (with micro-roughness $\sigma_{M1} = 0.5$ nm), as given by equation (4), produced by 92 superimposed diffraction profiles like the ones shown in Fig. 6. We work with the following assumptions:

- the light scattered by M1 is totally reflected by M2 and the mirrors of the second stage (see section 2.2.

- The scattering action of M2 and the mirrors of the second stage (see section 2.2) is negligible with respect to the scattering off M1, since it is scattering of scattered light.
- The light scattered by the telescope structure is negligible with respect to the contribution due to the diffraction from the PM apertures, because only the PM apertures are directly hit by the solar disk light.

Within these hypotheses, the stray light estimated on the primary focal plane is the same that we would obtain on the telescope focal plane. Figure 7 shows the resulting stray light pattern on the primary focal plane, in units normalized to the solar disk brightness as it would be imaged by M1 on its focal plane. In order to retrieve an

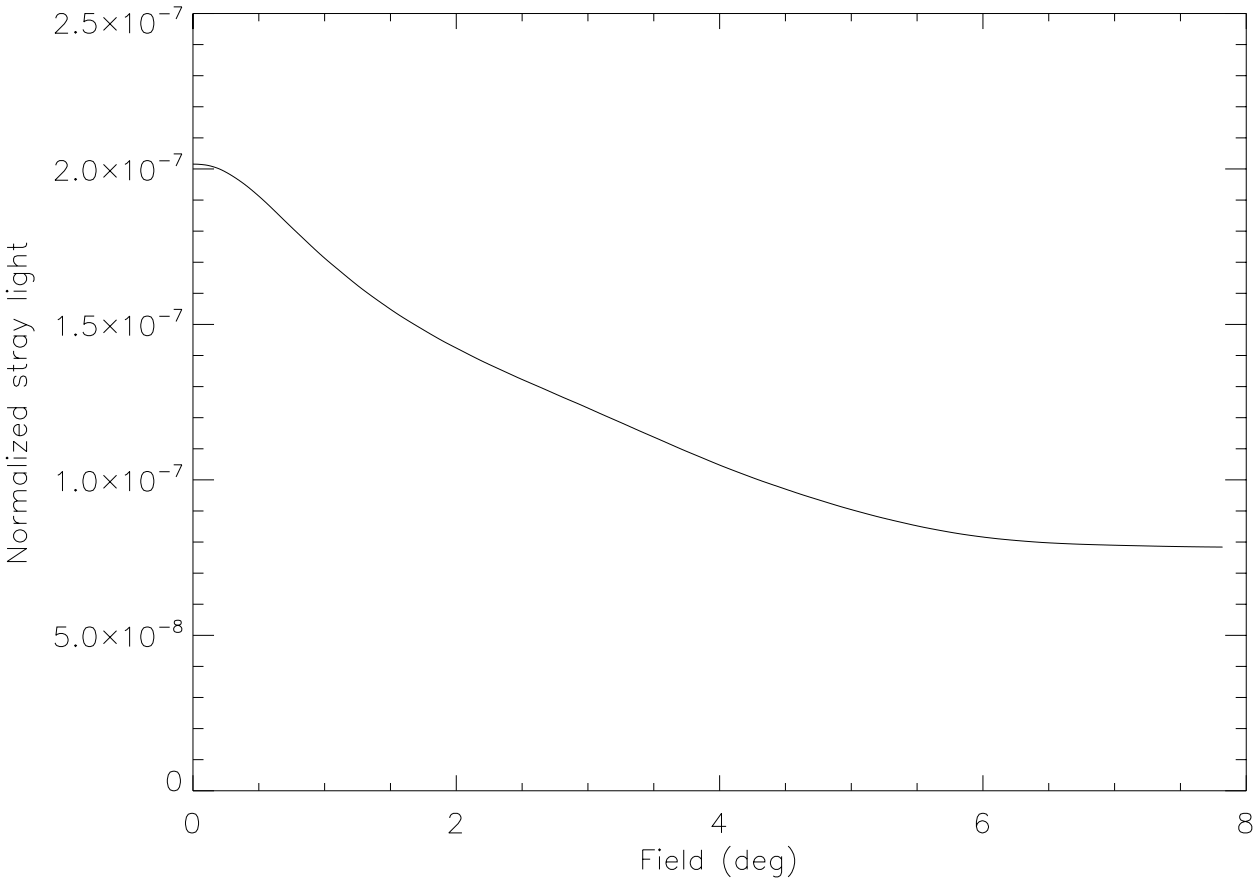

Figure 7. Stray light level on the primary focal plane.

absolute estimate to be compared with the expected signal, we consider the maximum of the curve of Fig. 7, $SL_{MAX} = 2 \times 10^{-7}$.
As an over-estimate, let's consider the stray light contribution constant over the wavelength range of AGP, $\Delta\lambda = 400 \div 800$ nm.
The stray light in absolute units would be then approximately given by:

$$I_{SL} = 92 \cdot A_{pup} \cdot SL_{MAX} \cdot \Delta\lambda \cdot I_{\odot} \cdot \frac{1}{\pi R_{\odot}^2} \cdot \frac{1}{\epsilon_{ph}} \simeq 0.01 \ \frac{\text{photo-electrons}}{\text{s arcsec}^2} \tag{5}$$

where A is the area of the single aperture on the PM (radius 10.7 mm), $I_{\odot} = 1.92$ $Wm^{-2}nm^{-1}$ is the solar irradiance at 500 nm,[15] $R_{\odot} = 960$ arcsec is the solar disk divergence and ϵ_{ph} is the energy of a photon at 500 nm.

It is a very low stray light level, which may allow to observe stars close to the Sun down to magnitudes fainter than V=17 mag.
However, it must be considered that it is a preliminary evaluation, performed with an ideal instrument. The only real ingredient that has been included in the evaluation is a standard surface roughness of the M1. For example, we did not consider the dust contamination, which can be among the major offenders in a coronagraphic instrument. The surface contamination of the M1 may lead to an increase of an order of magnitude of the stray light level on the focal plane. Another order of magnitude may be generated by irregularities or dust grains on the edges of the 92 entrance apertures, as it has been shown for the prototype of Solar Orbiter/METIS.[1]
The proposed design might therefore be considered as a conservative preliminary version, to be reviewed in a more detailed analysis including the above mentioned dust and roughness contributions, as well as optical component manufacturing and alignment aspects. Moreover, in-flight re-alignment and optical parameter deterioration due to the space environment conditions shall be considered in the design optimization.

4. CONCLUSIONS

The Astrometric Gravitation Probe is a space mission concept aimed at testing the General Relativity and competing gravitation theories by measurement of the light deflection and Solar System Ephemerides.
The astrometric goal of the mission will be accomplished by means of a coronagraphic design, characterized by 92 circular entrance apertures which help in dumping the solar disk light beyond the instrument, following the principle of the Solar Orbiter/METIS coronagraph inverted external occulter.[1]
The solar disk light diffracted by the 92 apertures and scattered by the telescope optics may generate a background stray light that prevent the observation of high magnitudes.
This paper describes a thorough preliminary analysis of the stray light as generated by diffraction and scattering. The analysis cannot be more than preliminar due to the relatively early stage of the mission concept, but it nevertheless gives important confirmations on the quality of the instrument design.
The estimated stray light level is 0.01 photo-electrons/s per square arcsec, which would allow to set a detection limit fainter than V=17 mag. It must in any case be considered that only ideal components were accounted for in our analysis, except for the micro-roughness of the primary mirror surface. The result could be considerably degraded by including further realistic aspects in the calculations, such as the dust contamination of the mirror surface or irregularities on the edges of the 92 entrance apertures. The inclusion of additional physical effects will be a crucial part of forthcoming design developments.

REFERENCES

[1] Landini, F., Romoli, M., Capobianco, G., Vives, S., Fineschi, S., Massone, G., Loreggia, D., Turchi, E., Guillon, C., Escolle, C., Pancrazzi, M., and Focardi, M., "Improved stray light suppression performance for the solar orbiter/METIS inverted external occulter," in [*Solar Physics and Space Weather Instrumentation V*], *Proc. SPIE* **8862**, 886204.1–19 (Sept. 2013).

[2] Will, C. M., "The Confrontation between General Relativity and Experiment," *Living Reviews in Relativity* **9** (Mar. 2006).

[3] Dyson, F. W., Eddington, A. S., and Davidson, C., "A Determination of the Deflection of Light by the Sun's Gravitational Field, from Observations Made at the Total Eclipse of May 29, 1919," *Philosophical Transactions of the Royal Society of London Series A* **220**, 291–333 (1920).

[4] Shapiro, S. S., Davis, J. L., Lebach, D. E., and Gregory, J. S., "Measurement of the Solar Gravitational Deflection of Radio Waves using Geodetic Very-Long-Baseline Interferometry Data, 1979 1999," *Physical Review Letters* **92**, 121101 (Mar. 2004).

[5] Bertotti, B., Iess, L., and Tortora, P., "A test of general relativity using radio links with the Cassini spacecraft," *Nature* **425**, 374–376 (Sept. 2003).

[6] Verma, A. K., Fienga, A., Laskar, J., Manche, H., and Gastineau, M., "Use of MESSENGER radioscience data to improve planetary ephemeris and to test general relativity," *A&A* **561**, A115 (Jan. 2014).

[7] Fienga, A., Laskar, J., Kuchynka, P., Manche, H., Desvignes, G., Gastineau, M., Cognard, I., and Theureau, G., "The INPOP10a planetary ephemeris and its applications in fundamental physics," *Celestial Mechanics and Dynamical Astronomy* **111**, 363–385 (Nov. 2011).

[8] Perryman, M. A. C., "Overview of the Gaia Mission," in [*Astrometry in the Age of the Next Generation of Large Telescopes*], Seidelmann, P. K. and Monet, A. K. B., eds., *Astronomical Society of the Pacific Conference Series* **338**, 3 (Oct. 2005).

[9] de Bruijne, J. H. J., "Science performance of Gaia, ESA's space-astrometry mission," *Astrophysics and Space Science* **341**, 31–41 (Sept. 2012).

[10] Müller, D., Marsden, R. G., St. Cyr, O. C., and Gilbert, H. R., "Solar Orbiter . Exploring the Sun-Heliosphere Connection," *Sol. Ph.* **285**, 25–70 (July 2013).

[11] van Casteren, J. and Novara, M., "BepiColombo mission," *Mem. SAIt* **82**, 394 (2011).

[12] Riva, A., Gai, M., Landini, F., Lazzarini, P., Tintori, M., Anselmi, A., Cesare, S., Busonero, D., Lattanzi, M. G., and Vecchiato, A., "AGP (Astrometric Gravitation Probe) Optical Design Report," *Proc. SPIE* **9907**, in press (2016).

[13] de Bruijne, J., Kohley, R., and Prusti, T., "Gaia: 1,000 million stars with 100 CCD detectors," in [*Space Telescopes and Instrumentation 2010: Optical, Infrared, and Millimeter Wave*], *Proc. SPIE* **7731**, 77311C (July 2010).

[14] Grupp, F., Prieto, E., Geis, N., Bode, A., Katterloher, R., Bodendorf, C., Penka, D., and Bender, R., "The EUCLID NISP tolerancing concept and results," in [*Space Telescopes and Instrumentation 2014: Optical, Infrared, and Millimeter Wave*], *Proc. SPIE* **9143**, 91432X (Aug. 2014).

[15] Cox, A. N., [*Allen's Astrophysical Quantities*], AIP press, Springer-Verlag, New York (2000).

[16] Born, M. and Wolf, E., [*Principles of Optics*], Cambridge University Press, Cambridge (2001).

[17] Stover, J. C., [*Optical scattering: measurement and analysis*], McGraw-Hill, Inc., New York (1990).

[18] Fineschi, S., Romoli, M., Hoover, R. B., Baker, P. C., Zukic, M., Kim, J., and Walker, A. B., "Stray light analysis of a reflecting UV coronagraph/polarimeter with multilayer optics," in [*X-Ray and Ultraviolet Polarimetry*], Fineschi, S., ed., *Proc. SPIE* **2010**, 78–92 (Feb. 1994).